# Supramolecular Activation of $S_8$ by Cucurbiturils in Water and Mechanism of Reduction to $H_2S$ by Thiols: Insights into Biological Sulfane Sulfur Trafficking

Arman C. Garcia, Lev N. Zakharov, Michael D. Pluth*

*Department of Chemistry and Biochemistry, Materials Science Institute, Knight Campus for Accelerating Scientific Impact, and Institute of Molecular Biology. University of Oregon. Eugene, Oregon, 97403-12532. United States*

*pluth@uoregon.edu

**ABSTRACT:** Reactive sulfur species (RSS) play critical roles in diverse chemical environments. Molecules containing sulfane sulfur ($S^0$) have emerged as key species involved in cellular redox buffering as well as RSS generation, translocation, and action. Using cucurbit[7]uril (CB[7]) as a model hydrophobic host, we demonstrate here that $S_8$ can be encapsulated to form a 1:1 host guest complex, which was confirmed by solution state experiments, mass spectrometry, and X-ray crystallography. The solid state structure of CB[7]/$S_8$ shows that the encapsulated $S_8$ is available to nucleophiles through the carbonyl portals of the host. Treatment of CB[7]/$S_8$ with thiols results in efficient reduction of $S_8$ to $H_2S$ in water at physiological pH. We establish that encapsulated $S_8$ is attacked by a thiol within the CB[7] host and that the resultant soluble hydropolysulfide is ejected into solution, where it reacts further with thiols to generate soluble sulfane sulfur carriers and ultimately $H_2S$. The formation of these intermediate is supported by observed kinetic saturation behavior, competitive inhibition experiments, and alkylative trapping experiments. We also demonstrate that CB[7]/$S_8$ can be used to increase sulfane sulfur levels in live cells using fluorescence microscopy. More broadly, this work suggests a general activation mechanism of $S_8$ by hydrophobic motifs, which may be applicable to proteins, membranes, or other bimolecular compartments that could transiently bind and solubilize $S_8$ to promote reaction with thiols to solubilize and shuttle $S_8$ back into the redox labile sulfane sulfur pool. Such a mechanism would provide an attractive manifold in which to understand the RSS translocation and trafficking.

## Introduction

Reactive sulfur species (RSS) play critical roles in diverse chemical environments ranging from biological chemistry to global sulfur cycles.[1-2] This importance is even reflected in terrestrial evolution, with early chemoautotrophic sulfur-reducing microbes using oxidized forms of sulfur as electron acceptors to generate $H_2S$ and $CO_2$ when Earth's atmosphere was much more reducing.[3] Remnants of our sulfur-reliant past are found in contemporary biology in our mitochondria, which likely evolved from a symbiotic fusion between sulfide-oxidizing α-protobacteria and sulfur-reducing archaea.[4-6] Building from this evolutionary importance, interest in biological RSS has been reinvigorated in the last two decades, in part due to the discovery that hydrogen sulfide ($H_2S$) is an endogenously produced signaling molecule.[7-11] $H_2S$ joins nitric oxide (NO) and carbon monoxide (CO) in a group of endogenous gaseous molecules often referred to as gasotransmitters.[12] $H_2S$ is now accepted to play key roles in diverse signaling and regulatory pathways and has been investigated extensively as both a research tool and potential therapeutic agent in different diseases affecting the cardiovascular, neuronal, gastrointestinal, and other systems.[13-14]

The chemical mechanisms by which $H_2S$ exerts biological action is intrinsically tied to a complex and interconnected array of RSS. Although sulfur can access oxidation states from -2 to +6 in biology,[15] much of established RSS redox and signaling occurs within the fully reduced ($S^{2-}$) to the sulfane sulfur ($S^0$) state. Common entities within this 2 electron redox manifold include $H_2S$, thiols, persulfides (RSSH), organic hydropolysulfides ($RS(S)_nSH$), and organic / inorganic polysulfides ($RS(S)_nSR$, $HS(S)_nSH$). These and related sulfane sulfur containing compounds form a redox-labile RSS pool with key roles in diabetes mellitus, high blood pressure, schizophrenia, as well as other diseases.[14, 16-17] Redox-labile RSS with $S^{1-}$ or $S^0$ oxidation states often generate species with enhanced reactivity, which highlights why this pool of compounds may be particularly important in cellular signaling processes. As an example, persulfidation of protein Cys residues is a key oxidative post-translational modification that can modify protein activity and also that protects proteins from irreversible oxidation during aging.[18] More broadly, this pool of soluble

sulfane sulfur containing species plays key and emerging roles in cellular redox buffering as well as RSS generation, translocation, and action.

In parallel with the rapidly expanding biological roles of RSS has been the development and application of chemical tools for the delivery of both fully reduced and sulfane sulfur species.[19-22] This work has led to significant advances in both the development of practical tools for RSS delivery and also in expanding fundamental RSS chemistry that informs on biological action. For example, small molecule RSS donors have shown high efficacy in animal models for conditions ranging from cardiovascular disease and ischemia/reperfusion injury to gastrointestinal inflammation and wound healing.[23-25] Similarly, contemporary investigations have led to the discovery of new fundamental chemistry of persulfides and polysulfides,[26-28] new approaches for responsive RSS delivery,[29-30] and new interconnectivities with other small signaling molecules.[31-35] An attractive approach for sulfane sulfur delivery would be to use systems with only $S^0$ atoms. A significant challenge with this approach, however, is that the simplest form of sulfane sulfur, $S_8$, is essentially insoluble in water (~1.96 x $10^{-8}$ M).[36] This solubility is significantly lower than the generally-accepted low micromolar levels of sulfane sulfur in cellular environments.[37-38] More broadly, combining the vibrant sulfane sulfur redox landscape with the low solubility of $S_8$ raises the yet unanswered question of why $S_8$ is not deposited or precipitated in mammalian organisms.

An emerging platform to address these questions and limitations is to use macrocyclic receptors as potential host molecules for $S_8$. Few prior reports have investigated the direct binding of $S_8$ to host molecules. In one example, a trigonal prismatic $Ag^+$ cage was demonstrated to bind $S_8$ in organic solution and in the solid state.[39] Closer inspection of the X-ray structure showed direct interactions between the $S^0$ atoms and the $Ag^+$ atoms in the host, which likely contributed as a driving force for encapsulation. In related example, a water-soluble $Pd^{2+}$ ligated polyaromatic host was used to bind different sulfur allotropes, as evidenced by mass spectrometry and X-ray analysis.[40] Neither of these above examples probed the reactivity of bound $S_8$ with additional reactants. In more recent work, we recently showed that the fully-organic 2-hydroxypropyl β-cyclodextrin (2HPβ) could also be used to solubilize $S_8$ in water. Using a 50 wt% solution of 2HPβ resulted in up to 2 mM $S_8$ in water, and the resultant 2HPβ/$S_8$ complex could be used to decrease $NO_2^-$ production in Raw 264.7 macrophage cells stimulated with proinflammatory lipopolysaccharides.[41] Similarly, treatment of isolated GAPDH enzyme with 2HPβ/$S_8$ modulates enzyme activity through sulfuration of a key GAPDH Cys residue.[42] Although both of these examples suggest that solubilized $S_8$ may be bioavailable, the mechanism of $S_8$ activation and the interplay between soluble sulfane sulfur species remains unclear. Understanding the mechanism by which complementary host molecules can solubilize and activate $S_8$ would provide important insights into the biological sulfur redox economy. Furthermore, these studies would advance our understanding of why $S_8$ is not a common deposited thermodynamic product in biological environments, even though small molecule polysulfides can extrude $S_8$ directly.[43] With the goal of advancing our understanding of these fundamental questions, we report here the use of a cucurbituril supramolecular host as a model system to provide a detailed mechanistic investigation into the binding, activation, and reduction of $S_8$ by hydrophobic host motifs (Figure 1).

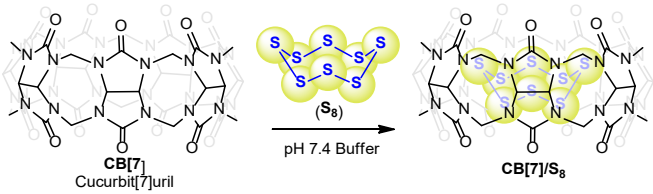


**Figure 1.** $S_8$ binding to cucurbit[7]uril in water.

## Results and Discussion

### *CB[7]/$S_8$ Binding and Characterization*

Macrocyclic receptors, such as calixarenes (CX), cyclodextrins (CD), and cucurbit[*n*]urils (CB[*n*]s) have been studied extensively due to their well-established host-guest chemistry and ability to bind different guests. CB[5,6,7,8,10] can be prepared by an acid-catalyzed condensation between glycouril and paraformaldehyde and have been used previously to increase the aqueous solubility and bioavailability of different biologically-relevant guests.[44-47] In particular, CB[*n*]s are particularly attractive hosts because of their discrete sizes, hydrophobic interiors, uniformity of functional groups around portal, water solubility, high binding affinity for hydrophobic guests, and high biocompatibility.[48-50]{Lorenzo, 2001 #37}{Cao, 2014 #38} Guest binding in CB[*n*]s is primarily driven by size compatibility of the CB[*n*] cavity and potential interactions of charged or hydrogen bonding motifs with the carbonyl portals. Because of these characteristics, we surmised that CB[*n*]s would be ideal hosts for $S_8$ based on the tunable size and potential for hydrogen bonding of incoming thiol nucleophiles to the CB[7] carbonyl-lined portals.

The structural rigidity of CB[*n*]s provides well-defined interior cavities that can be matched with specific guest to maximize host-guest size complementarity. Prior work has shown that both synthetic and biological host-guest structures maintain an ideal packing coefficient, defined as volume of the guest divided by the volume of the host cavity, of 0.55 ± 0.09.[51] Based on the volume of $S_8$ (~149 Å$^3$), we expected that CB[7] (~279 Å$^3$) would be an ideal host for $S_8$ based on the calculated packing coefficient of 0.53 for CB[7]/$S_8$. To test this hypothesis, we prepared CB[6], CB[7], and CB[8] using the Pellinger method,[52] and treated aqueous solution of each host in pH 7.4 PBS buffer with excess $S_8$ for 24 hours. After filtration of the heterogenous solutions, we measured the UV-Vis absorbance of each sample to determine whether $S_8$ ($\lambda_{max}$ = 263 nm; ε = 6730 $M^{-1}cm^{-1}$) had been solubilized.[53] As expected, we observed a significant increase in the $S_8$ absorbance for solutions of CB[7], whereas significant increases in $S_8$ absorbances were not observed for CB[6] or CB[8] (Figure S3). Using this method, we could readily solubilize 1.0 ± 0.3 mM $S_8$ in 20

mM solutions of CB[7], which is significantly more efficient than the 2 mM solubility of $S_8$ in 50% w/w (~360 mM) solutions of 2HP⍰ from prior work.[41]

Having established that $S_8$ can be solubilized by CB[7], we next set to measure the binding affinity ($K_a$) and binding stoichiometry. Because of the low solubility of $S_8$ in water and lack of distinct spectroscopic signals for free and bound $S_8$, we used constant activity method to measure the $K_a$ for $S_8$ binding to CB[7].[54] In this method, the total $S_8$ in solution ($S_t$) was measured as a function of increasing CB[7] concentration (0.25-1.5 mM) in the presence of excess $S_8$. The presence of solid $S_8$ ensures that the activity of $S_8$ in free solution remains constant at different CB[7] concentrations. Under these conditions, the concentration of $S_8$ bound in CB[7] is equal to $S_t - s_o$, where $s_o$ is the solubility of $S_8$ in water ($1.96 \times 10^{-8}$ M). Using this method, eq 1 can be used to measure $K_a$ for binding from the *y*-intercept, and also the binding stoichiometry ($n$) from the slope of the plot.

$$\log\frac{S_t - s_o}{s_o} = \log K_a + n\log[\mathrm{CB[7]}] \qquad \text{eq (1)}$$

The resultant log-log plot of $(S_t - s_o)/s_o$ versus [CB[7]] provided a linear plot with a slope of 0.99, which is consistent with 1:1 host-guest binding (Figure 2). In addition, the *y*-intercept afforded $\log(K_a) = 7.06 \pm 0.22$, which is significantly higher than the prior $S_8$ binding in the 2HPβ/$S_8$ system. In further support of 1:1 binding in solution, we also measured the ESI-MS spectrum of an aqueous solution of CB[7]/$S_8$, which showed a peak at 710.0673 m/z ($[\mathrm{CB[7]} + S_8 + 2H^+]^{2+}$, which matches the expected exact mass of 710.0673 m/z and isotopic distribution expected for the CB[7]/$S_8$ complex (Figure S4). Taken together, these measurements support formation of a 1:1 host-guest complex between $S_8$ and CB[7].

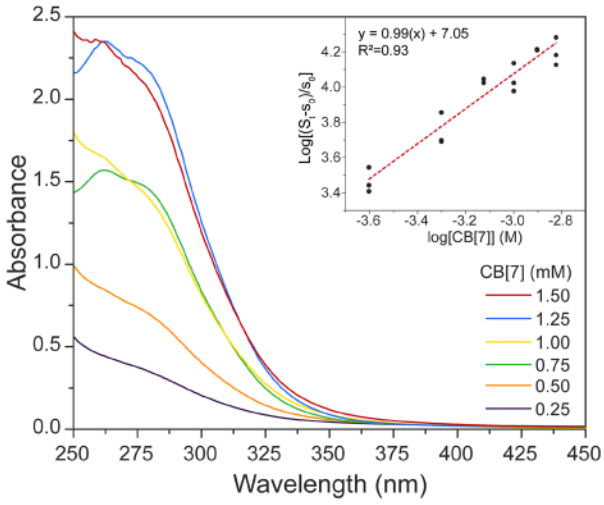


**Figure 2.** UV-vis spectra of the absorbance of CB[7]/$S_8$ with increasing concentrations of CB[7] (0.25-1.50 mM) in the presence of excess $S_8$. Inset: Log-log plot for binding constant and binding stoichiometry of $S_8$ in CB[7].

Further supporting formation of a 1:1 host-guest complex, we grew crystals suitable for single-crystal X-ray diffraction by slow evaporation of a saturated aqueous solution of CB[7]/$S_8$ using molecular sieves to increase the rate of evaporation. The resultant host guest complex crystallized in $Pca2_1$ with 4 CB[7]/$S_8$ molecules per asymmetric unit and 16 molecules in the unit cell (Figure 3). Each $S_8$ molecule is fully encapsulated in a CB[7] host, and bound $S_8$ is accessible to solvent through the carbonyl portals. Notably, the $S_8$ ring is perpendicular to the CB[7] macrocycle, rather the expected coaxial orientation, which leads to significant host elongation (*vide infra*). Because none of the CB[7] or $S_8$ molecules sit on a special position in the orthorhombic space group, the incommensurate symmetry of the CB[7] and $S_8$ does not lead to symmetry-generated disorder within the unit cell. Each of the 4 crystallographically distinct CB[7]/$S_8$ molecules are well-ordered within the structure and both host and guest have well-defined thermal parameters.

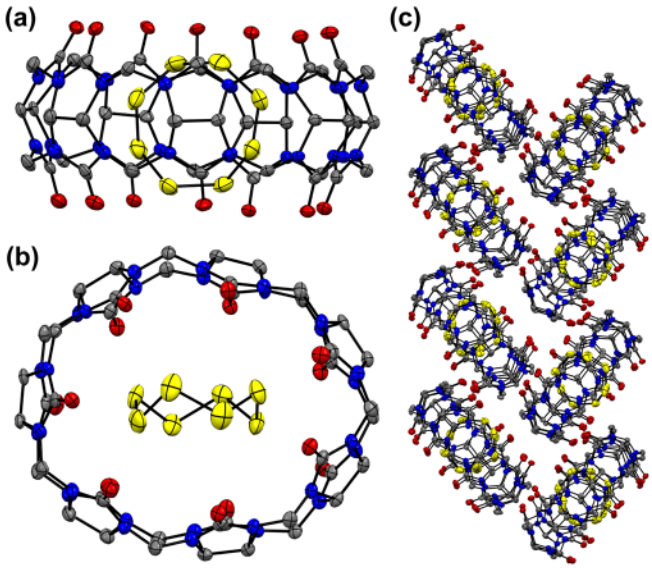


**Figure 3.** (a) Side on and (b) top view of the molecular structure of CB[7]/$S_8$. (c) Unit cell packing viewed down the b-axis showing the CB[7]/$S_8$ herringbone alignment. Ellipsoids are shown at 50% probability levels. Red, grey, blue, and yellow ellipsoids represent O, C, N, and S, respectively. Hydrogen atoms and solvent molecules are omitted for clarity.

When examining the molecular structure more closely, we noticed that each CB[7] in the CB[7]/$S_8$ structure is significantly distorted from circularity. To better understand the magnitude of this distortion, we first measured the shortest and longest radii of the CB[7] by calculating the centroid of each CB[7] defined by the 14 $sp^3$ glycouril carbons and measuring the distance between the centroid and each of the 14 $sp^3$ carbons. Comparing these radii showed shortest and longest values of 5.47 and 6.20 Å, respectively ($\Delta_r = 0.73$ Å). We next calculated the mathematical ellipticity, or deviation from circularity, for each CB[7] to better compare with other CB[7] host-guest complexes (See SI for discussion and methods). In our analysis of prior CB[7] host-guest complexes, we limited our search

to CB[7] structures in which the guest was fully encapsulated within the host cavity. We excluded structures in which the guest interacted directly with the carbonyl portal or with the exterior of the CB[7] host, since these structures may result in additional intermolecular forces contributing to host deformation. To benchmark the normal ellipticity of "empty" CB[7], we used data from published X-ray structures of CB[7] that either had no guest or that only contained solvent molecules within the cavity. These measurements also help to account for normal distortions that may arise from crystal packing forces in the solid state structures. We measured centroids and individual radii as described above for each structure (Table S1). Working under the assumption that the perimeter of each CB[7] was identical due to the uniformity of covalent bond distances in the glycouril subunits, we used the above radius measurements to calculate the mathematical ellipticity of each CB[7] host. On the basis of this analysis, we found that the average ellipticity for 'empty' CB[7] was 0.064 ± 0.037, which was not statistically different from the prior CB[7] host guest complexes (0.066 ± 0.031). By contrast, the average ellipticity of the 4 CB[7] molecules in the CB[7]/$S_8$ host-guest complexes was 0.14 ± 0.02, which is significantly more distorted. Closer analysis of the structure shows that this structural deviation of the CB[7] host leaves two sulfur atoms on each face of the CB[7]/$S_8$ complex accessible to solvent or nucleophiles, which provides a key structural insight into how $S_8$ can be activated by thiol-based nucleophiles in solution (*vide infra*).

*Bioavailability CB[7]/$S_8$*

Because CB[7] has been used previously to deliver encapsulated guests in cellular environments,[55-57] we were curious whether CB[7]/$S_8$ could be used to deliver $S_8$ and increase sulfane sulfur levels in live cells.[58] To test this directly, we used the sulfane-sulfur responsive fluorescent probe SSP4 to determine whether intracellular $S^0$ levels were modified by treatment with CB[7]/$S_8$ (Figure 4).[59] We incubated HeLa cells with either CB[7] (10 μM), $K_2S_X$ (100 μM), or CB[7]/$S_8$ (80 μM $S^0$) for 5 hours and then washed the cells and replaced the media to remove any extracellular species. After subsequent treatment with 20 μM SSP4 and further incubation for 15 minutes, the cells were washed again and the media was replaced prior to fluorescence imaging. Treatment of HeLa cells with CB[7] alone did not result in an increase in SSP4 fluorescence, which confirms that CB[7] alone does not increase intracellular $S^0$ levels. By contrast, treatment with CB[7]/$S_8$ resulted in a significant increase in SSP4 fluorescence, which matched the positive sulfane sulfur control experiment using $K_2S_x$. These data demonstrate that CB[7]/$S_8$ is can effectively deliver sulfane sulfur to live cells, which highlighting the generality and biocompatibility of using CB[7] for $S_8$ delivery.

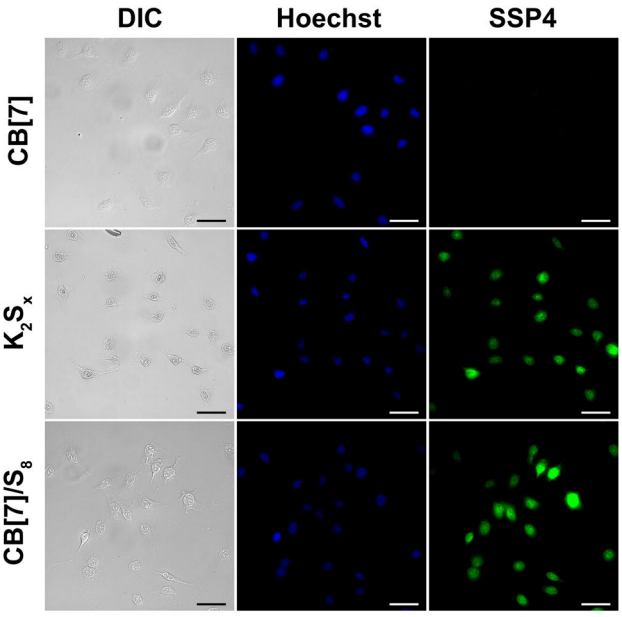


**Figure 4.** Fluorescent images of sulfane sulfur in live HeLa cells using the SSP4 fluorescent probe. Cells were treated with either CB[7] (10 μM), $K_2S_X$ (100 μM), or CB[7]/$S_8$ (80 μM $S^0$). Scale bar = 50 μm.

*CB[7]/$S_8$ Reactivity and Thiol Activation Mechanism*

Having established both the molecular structure and biological compatibility of CB[7]/$S_8$, we next investigated the chemical accessibility of the bound $S_8$ toward thiol-based reductants to generate $H_2S$. A small library of biologically-relevant and water soluble thiols were used to probe the chemical accessibility and activation of bound $S_8$. We initially aimed to use the methylene blue (MB) assay measuring released $H_2S$,[60] but we found that the MB dye produced upon reaction with $H_2S$ is encapsulated in CB[7], which prohibited use of this common approach (Figure S5).[58] To overcome this challenge, we used a Unisense $H_2S$ responsive electrode to measure $H_2S$ concentrations. In addition to providing a real-time response with no sample workup, the electrode is also significantly more sensitive for $H_2S$ than the MB assay.

Because reduction of each $S^0$ atom to $H_2S$ requires two equivalents of thiol, we started our investigations with the 1,4-dithiothreitol (DTT) to simplify the reaction. As expected, treatment of CB[7]/$S_8$ (80 μM $S^0$) with DTT resulted in quantitative reduction of the bound $S_8$ to $H_2S$ over the course of 90 minutes (Figure 5). Similarly, treatment of CB[7]/$S_8$ with biologically-relevant thiols, such as cysteine (Cys), glutathione (GSH), or homocysteine (Hcy), also resulted in efficacious reduction of $S_8$ to $H_2S$, (56-69% over 90 min). In comparison, *N*-acetyl cysteine (NAC) and penicillamine (PEN) are far less reactive toward CB[7]/$S_8$. Using the above data, we fit the resultant $H_2S$ release curves to measure $k_{obs}$ for each thiol to determine whether thiol or thiolate was the active nucleophile. If the thiolate is the active nucleophile in $S_8$ activation, then we would expect to observe an inverse relationship between $k_{obs}$ and thiol p$K_a$. As expected, the resulting plot of log($k_{obs}$) versus

log(p$K_a$) was linear, with more acidic thiols resulting in faster $S_8$ reduction from CB[7]/$S_8$, which is consistent with thiolate being the active nucleophile in solution (Figure S6). Closer inspection of the $H_2S$ generation curves for the series of thiols above shows immediate $H_2S$ production in the case of DTT, whereas treatment with other thiols result in a brief induction period. This induction period suggests that an intermediate required for $H_2S$ generation may initially accumulate during the thiol-mediated reduction process.

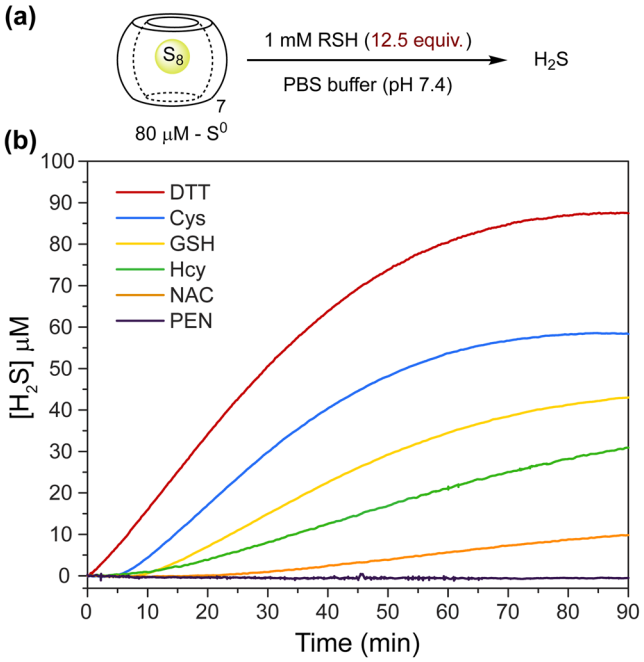


**Figure 5**. (a) Reaction conditions for thiol-triggered release of $H_2S$ from CB[7]/$S_8$. (b) $H_2S$ release from CB[7]/$S_8$ (80 μM $S^o$) in the presence of different thiols. The experiments were performed in triplicate.

To better understand the mechanism of $S_8$ reduction by thiols in CB[7]/$S_8$ we envisioned two primary mechanisms. Both mechanisms start with initial thiolate attack on the encapsulated $S_8$ to open the $S_8$ ring to form a thiol-bound hydropolysulfide (RS-$S_8$H) (Figure 6). In Mechanism I, the resultant RS-$S_8$H remains encapsulated in the CB[7], and subsequent reduction steps occur within the host. By contrast, in Mechanism II, the RS-$S_8$H intermediate in ejected from the CB[7], and each subsequent reduction step happens in solution. In both mechanisms, $S_8$ reduction and subsequent $H_2S$ formation should show a rate dependence on thiol concentration, but would show saturation behavior if the initial thiol attack on the CB[7]/$S_8$ was no longer rate limiting at high thiol concentration.

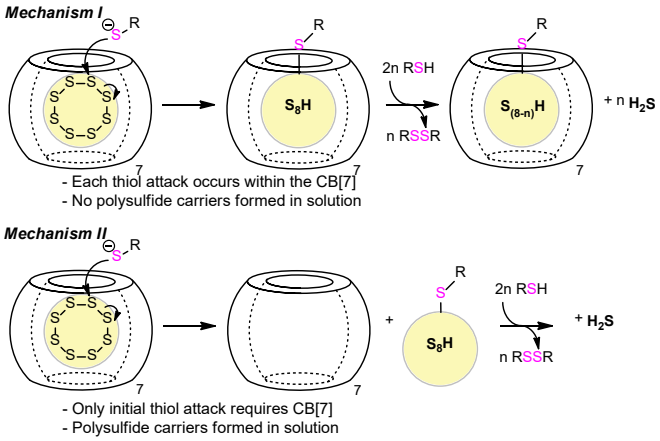


**Figure 6.** Propose mechanisms for reduction of $S_8$ in CB[7]/$S_8$ by thiols to generate $H_2S$. Mechanism I proceeds through polysulfide carries within the CB[7] host, whereas Mechanism II generates polysulfide carriers in solution.

To test these scenarios, we measured $H_2S$ production from CB[7]/$S_8$ (80 μM $S^o$) under pseudo first order conditions with increasing concentrations of Cys as the model thiol substrate (Figure 7). As expected, a plot of log($k_{obs}$) vs log([Cys]) was initially linear, but showed saturation behavior at concentrations above 10 mM Cys (Figure 7b). These results suggest that at high [Cys], attack of Cys on CB[7]/$S_8$ is rate limiting and once the resultant polysulfides are formed they are quickly reduced to $H_2S$. At lower [Cys], however, the rates of Cys attack on CB[7]/$S_8$ and the rate of reduction of the resultant polysulfides are competitive, which leads to the observed [Cys] dependence. In addition, increased [Cys] abolished the induction period for $H_2S$ formation (Figure 7a). Taken together, these data suggest that at low [Cys], polysulfide carriers accumulate prior to further reduction by Cys to generate $H_2S$, whereas at high [Cys], the formed polysulfide carriers are reduced to $H_2S$ immediately upon formation.

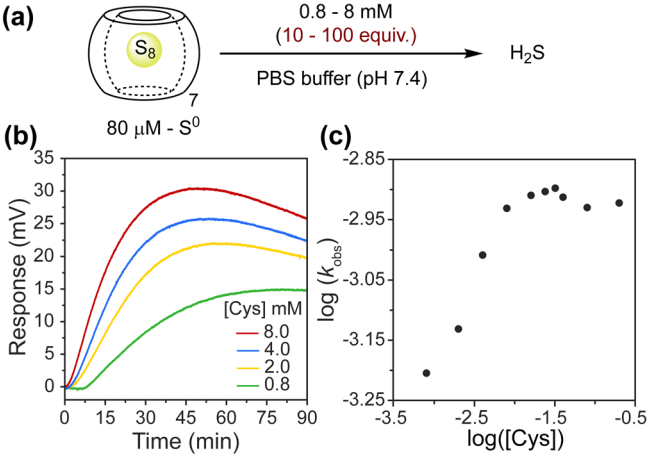


**Figure 7.** (a) Reaction scheme of thiol-dependent $H_2S$ release from CB[7]/$S_8$ (b) Representative $H_2S$ response upon treatment of CB[7]/$S_8$ (80 μM $S^o$) with increasing [Cys] (0.8-8 mM). (c) The plot of log($k_{obs}$) vs log[Cys] show saturation behavior.

To further investigate the role of CB[7] and potential intermediates formed during the thiol-mediated reduction of $S_8$ from CB[7]/$S_8$ we performed a series of experiments using proflavine (Pro) as a competitive guest ($K_a$ = 1.65 x10$^7$ M$^{-1}$).[61] To differentiate between Mechanism I and Mechanism II, we added Cys (1 mM) and increasing concentration of Pro (0-4 mM) to a solution of CB[7]/$S_8$ (80 μM S$^o$) and monitored $H_2S$ production. If the $H_2S$ generating steps of $S_8$ reduction are occurring solely within the CB[7] (Mechanism I), then we would expect increasing [Pro] to provide a dose-dependent decrease in the rate of $H_2S$ production (Figure 8a). Conversely, if the $H_2S$ generating steps of $S_8$ reduction are occurring outside of CB[7] (Mechanism II), then the initial rates of $H_2S$ production should be identical because they reflect polysulfide reduction in solution, which is a CB[7] independent process. The total $H_2S$ generated, however, should decrease with increasing [Pro] because there would be less initial CB[7]/$S_8$ in solution (Figure 8b).

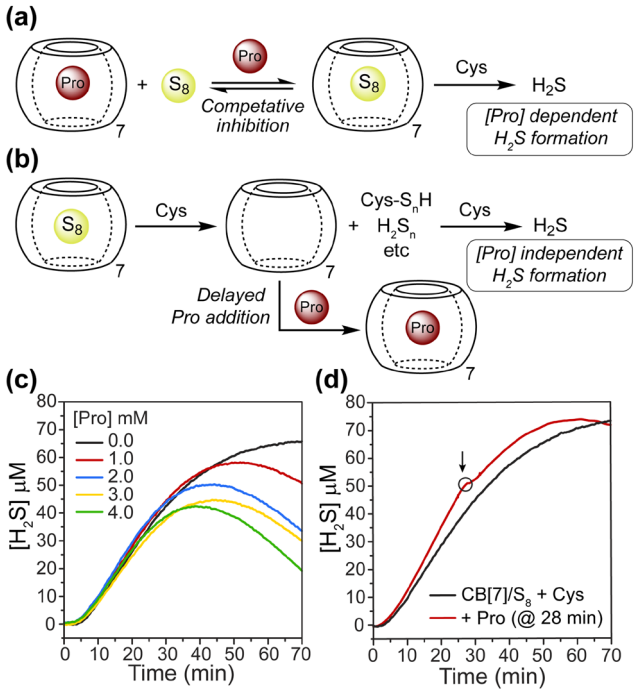


**Figure 8.** (a) Treatment of CB[7]/$S_8$ with proflavine (Pro) would decrease the rate of $H_2S$ production if each $H_2S$-generating step occurs within CB[7]. (b) Treatment of CB[7]/$S_8$ with Pro would not impact $H_2S$ release if free polysulfides are the resting intermediate. (c) Measured $H_2S$ production from CB[7]/$S_8$ (80 μM S$^o$) with Cys (1 mM) with increasing [Pro] (0-4 mM). (d) $H_2S$ production in unchanged when Pro is added during the course of the reaction of CB[7]/$S_8$ (80 μM S$^o$) with Cys (1 mM), confirming that polysulfides are the resting intermediate.

When performing these experiments, we observed identical initial $H_2S$ production rates but overall decreased $H_2S$ production with increasing [Pro], which is consistent with Mechanism II (Figure 8c). In a complementary experiment, we initiated the reaction of CB[7]/$S_8$ (80 μM S$^o$) with Cys (1 mM) and added excess Pro midway through the reaction. If the CB[7] is required for each step in $H_2S$ generation (ie Mechanism I), then we would expect to observe an immediate halt in $H_2S$ production upon Pro addition. If, however, CB[7] is only required for the initial step for $S_8$ activation and free polysulfides and related soluble sulfane sulfur carriers are the resting intermediate for the reaction (ie Mechanism II), then we would not expect to observe any change in $H_2S$ production upon Pro addition. Under these conditions, addition of Pro 28 minutes after Cys addition did not significantly change $H_2S$ production when compared the identical experiment without Pro addition, which again supports Mechanism II (Figure 8d). When taken together, these experiments confirm that the CB[7] is only required for the initial $S_8$ activation step and that polysulfides and other soluble sulfane sulfur carriers are the resting intermediates for the observed reduction chemistry.

If Mechanism II is the primary pathway for $H_2S$ formation, then we expect that polysulfides and related soluble S$^o$-containing RSS are formed during the reaction. We next investigated whether these RSS intermediates could be trapped by using the fluorescent alkylating agent monobromobimane (mBB).[62-63] Depending on the RSS species present, quenching with mBB results in different products, which can be differentiated by HPLC. For example, $H_2S$ and inorganic polysulfides react with 2 equiv. of mBB to produce sulfide dibimane or doubly-labeled polysulfides, respectively, whereas other sulfhydryl-containing species such as persulfides, organic hydropolysulfides, react with 1 equiv. of mBB to generate singly-labeled fluorescent derivatives. Based on this expected reactivity, we treated CB[7]/$S_8$ (80 μM S$^o$) with Cys (1 mM), allowed the reaction to proceed for 30 min, quenched the reaction with excess mBB, and analyzed the resultant products by HPLC (Figure 9). When comparing the resulting chromatogram with those from control experiments for mBB trapping of $H_2S$, persulfides, and polysulfides, we observe clear formation of $H_2S$ and polysulfides, further confirming the generation of free sulfane-sulfur carries in solution.

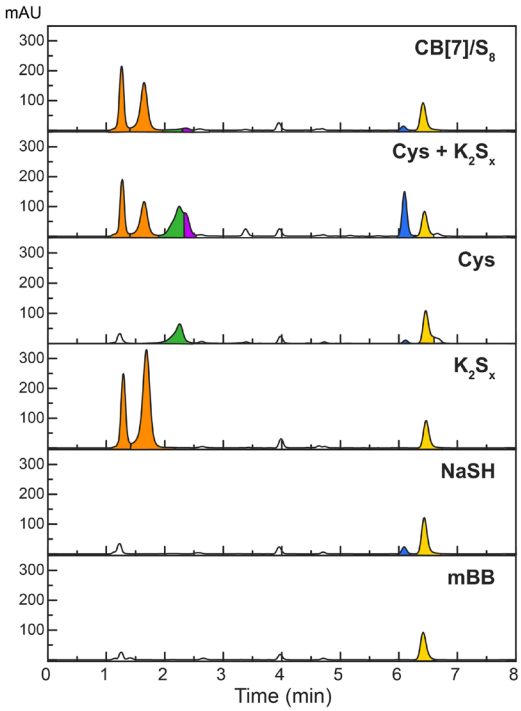


**Figure 9.** HPLC traces for CB[7]/$S_8$ the reaction of CB[7]/$S_8$ treated with Cys and quenched with mBB. Comparisons with background trapping reactions show significant formation of organic and inorganic polysulfides formed during the reaction.

Combining the above investigations allows for a more comprehensive mechanism of $S_8$ activation by CB[7] (Figure 10). $S_8$ is encapsulated in CB[7] in water to form the CB[7]/$S_8$ complex. The structure of the CB[7] allows for thiolate to access and attack the bound $S_8$ and eject soluble sulfane sulfur carriers in solution. These carriers then react further with thiols to generate other sulfane sulfur containing RSS, including inorganic polysulfides as well as Cys-ligated organic polysulfides and hydropolysulfides. Each of these classes of sulfane sulfur carriers has been implicated previously in the roles of sulfane sulfur action and translocation in cellular environments.[37, 64-65] In the presence of excess thiol or other reducing agents, the sulfane sulfur atoms in these carriers will be reduced fully to $H_2S$.

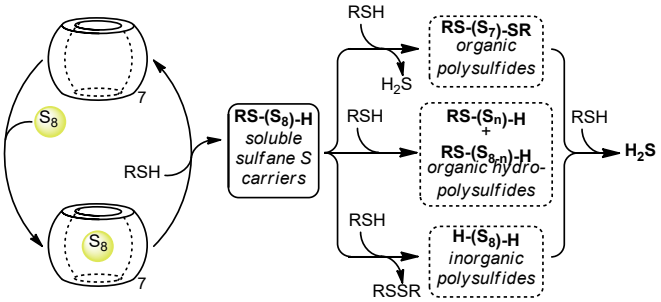


**Figure 10**. Mechanism of $S_8$ activation by CB[7] to generate soluble sulfane sulfur carriers en route to $H_2S$ generation.

More broadly, this determined mechanism provides an attractive manifold for the general activation of $S_8$ by hydrophobic motifs to generate redox-labile soluble sulfane sulfur carriers. Based on the dynamic sulfur redox economy in all living organisms, why is $S_8$ formation and subsequent precipitation not observed in cellular environments under physiological conditions? An attractive hypothesis is that available hydrophobic motifs, whether they be in proteins, membranes, or other bimolecular compartments, may transiently bind and solubilize $S_8$ to promote reduction by GSH or Cys to solubilize and shuttle $S_8$ back into the redox labile sulfane sulfur pool. Such a mechanism would provide an attractive manifold in which to understand the translocation and trafficking of RSS in complex redox environments.

## Conclusion

Sulfane sulfur is a key component of the redox labile sulfur pool, yet $S_8$ is insoluble in water and inaccessible to common thiol-mediated redox chemistry. We demonstrated that $S_8$ can be bound and solubilized in water using a CB[7] supramolecular host and that this solubilized form of $S_8$ can increase sulfane sulfur levels in live cells. The structure of the CB[7]/$S_8$ complex was determined by X-ray crystallography and confirmed that $S_8$ binds within the CB[7] cavity with a 1:1 stoichiometry. Treatment of the CB[7]/$S_8$ complex with thiols resulted in $S_8$ reduction to $H_2S$ with high efficiency and a linear dependence of $H_2S$ production rate on thiol p$K_a$. Furthermore, saturation behavior for $H_2S$ production was observed for thiols and competitive inhibition studies using proflavine demonstrated that only the initial thiol attack on the $S_8$ occurs within the CB[7] cavity and that soluble sulfane sulfur carriers are formed in solution. Alkylative trapping experiments with mBB further supported the formation of polysulfide and hydropolysulfide intermediates. In addition to expanding the supramolecular chemistry of $S_8$ as a biologically-relevant guest, the mechanistic work provides a useful paradigm for understanding $S_8$ uptake and activation by hydrophobic motifs and the interplay of $S_8$ with the redox labile sulfane sulfur pool.

## ASSOCIATED CONTENT

**Supporting Information**. Experimental procedures, compound characterization, and supplemental data. Crystallographic data is available through the CCDC 2175022. This material is available free of charge via the Internet at http://pubs.acs.org.

## AUTHOR INFORMATION

### Corresponding Author

* pluth@uoregon.edu

## ACKNOWLEDGMENT

This work was supported by the NSF (CHE-2004150). Microscopy instrumentation was supported by the NSF (CHE-1531189). We thank Dr. Sarah Bolton for initial experiments with CB[7]/$S_8$ and related systems.

## REFERENCES


1. Jørgensen, B. B.; Findlay, A. J.; Pellerin, A., The Biogeochemical Sulfur Cycle of Marine Sediments. *Front. Microbiol* **2019,** *10*, 849.
2. Rasch, P. J.; Barth, M. C.; Kiehl, J. T.; Schwartz, S. E.; Benkovitz, C. M., A description of the global sulfur cycle and its controlling processes in the National Center for Atmospheric Research Community Climate Model, Version 3. *Journal of Geophysical Research: Atmospheres* **2000,** *105* (D1), 1367-1385.
3. Olson, K. R.; Straub, K. D., The Role of Hydrogen Sulfide in Evolution and the Evolution of Hydrogen Sulfide in Metabolism and Signaling. *Physiology* **2016,** *31* (1), 60-72.
4. Embley, T. M.; Martin, W., Eukaryotic evolution, changes and challenges. *Nature* **2006,** *440* (7084), 623-630.
5. Szklarczyk, R.; Huynen, M. A., Mosaic origin of the mitochondrial proteome. *PROTEOMICS* **2010,** *10* (22), 4012-4024.
6. Olson, K. R.; Donald, J. A.; Dombkowski, R. A.; Perry, S. F., Evolutionary and comparative aspects of nitric oxide, carbon monoxide and hydrogen sulfide. *Respir. Physiol. Neurobiol.* **2012,** *184* (2), 117-129.
7. Abe, K.; Kimura, H., The possible role of hydrogen sulfide as an endogenous neuromodulator. *J. Neurosci.* **1996,** *16* (3), 1066-1071.
8. Yang, G. D.; Wu, L. Y.; Jiang, B.; Yang, W.; Qi, J. S.; Cao, K.; Meng, Q. H.; Mustafa, A. K.; Mu, W. T.; Zhang, S. M.; Snyder, S. H.; Wang, R., $H_2S$ as a physiologic vasorelaxant: Hypertension in mice with deletion of cystathionine gamma-lyase. *Science* **2008,** *322* (5901), 587-590.
9. Zanardo, R. C. O.; Brancaleone, V.; Distrutti, E.; Fiorucci, S.; Cirino, G.; Wallace, J. L., Hydrogen sulfide is an endogenous modulator of leukocyte-mediated inflammation. *Faseb J.* **2006,** *20* (12), 2118-2120.
10. Papapetropoulos, A.; Pyriochou, A.; Altaany, Z.; Yang, G. D.; Marazioti, A.; Zhou, Z. M.; Jeschke, M. G.; Branski, L. K.; Herndon, D. N.; Wang, R.; Szabo, C., Hydrogen sulfide is an endogenous stimulator of angiogenesis. *Proc. Natl. Acad. Sci. USA* **2009,** *106* (51), 21972-21977.
11. Bucci, M.; Papapetropoulos, A.; Vellecco, V.; Zhou, Z. M.; Pyriochou, A.; Roussos, C.; Roviezzo, F.; Brancaleone, V.; Cirino, G., Hydrogen Sulfide Is an Endogenous Inhibitor of Phosphodiesterase Activity. *Arterioscler. Thromb. Vasc. Biol.* **2010,** *30* (10), 1998-U254.
12. Wang, R., Two's company, three's a crowd: can H2S be the third endogenous gaseous transmitter? *The FASEB Journal* **2002,** *16* (13), 1792-1798.
13. Chen, W.-L.; Niu, Y.-Y.; Jiang, W.-Z.; Tang, H.-L.; Zhang, C.; Xia, Q.-M.; Tang, X.-Q., Neuroprotective effects of hydrogen sulfide and the underlying signaling pathways. *Reviews in the Neurosciences* **2015,** *26* (2), 129-142.
14. Ida, T.; Sawa, T.; Ihara, H.; Tsuchiya, Y.; Watanabe, Y.; Kumagai, Y.; Suematsu, M.; Motohashi, H.; Fujii, S.; Matsunaga, T.; Yamamoto, M.; Ono, K.; Devarie-Baez, N. O.; Xian, M.; Fukuto, J. M.; Akaike, T., Reactive cysteine persulfides and S-polythiolation regulate oxidative stress and redox signaling. *Proceedings of the National Academy of Sciences* **2014,** *111* (21), 7606-7611.
15. Lau, N.; Pluth, M. D., Reactive sulfur species (RSS): persulfides, polysulfides, potential, and problems. *Curr. Opin. Chem. Biol.* **2019,** *49*, 1-8.
16. Kunikata, H.; Ida, T.; Sato, K.; Aizawa, N.; Sawa, T.; Tawarayama, H.; Murayama, N.; Fujii, S.; Akaike, T.; Nakazawa, T., Metabolomic profiling of reactive persulfides and polysulfides in the aqueous and vitreous humors. *Scientific Reports* **2017,** *7* (1), 41984.
17. Rajpal, S.; Katikaneni, P.; Deshotels, M.; Pardue, S.; Glawe, J.; Shen, X.; Akkus, N.; Modi, K.; Bhandari, R.; Dominic, P.; Reddy, P.; Kolluru, G. K.; Kevil, C. G., Total sulfane sulfur bioavailability reflects ethnic and gender disparities in cardiovascular disease. *Redox Biology* **2018,** *15*, 480-489.
18. Wilkie, S. E.; Borland, G.; Carter, R. N.; Morton, N. M.; Selman, C., Hydrogen sulfide in ageing, longevity and disease. *Biochemical Journal* **2021,** *478* (19), 3485-3504.
19. Szabo, C.; Papapetropoulos, A., International Union of Basic and Clinical Pharmacology. CII: Pharmacological Modulation of $H_2S$ Levels: $H_2S$ Donors and $H_2S$ Biosynthesis Inhibitors. *Pharmacol. Rev.* **2017,** *69* (4), 497-564.
20. Powell, C. R.; Dillon, K. M.; Matson, J. B., A review of hydrogen sulfide ($H_2S$) donors: Chemistry and potential therapeutic applications. *Biochem. Pharmacol* **2018,** *149*, 110-123.
21. Levinn, C. M.; Cerda, M. M.; Pluth, M. D., Activatable Small-Molecule Hydrogen Sulfide Donors. *Antioxid. Redox Signal.* **2020,** *32* (2), 96-109.
22. Dillon, K. M.; Matson, J. B., A Review of Chemical Tools for Studying Small Molecule Persulfides: Detection and Delivery. *ACS Chem. Biol.* **2021,** *16* (7), 1128-1141.
23. Kolluru, G. K.; Shen, X.; Kevil, C. G., Reactive Sulfur Species. *Arteriosclerosis, Thrombosis, and Vascular Biology* **2020,** *40* (4), 874-884.
24. Zhao, Y.; Bhushan, S.; Yang, C.; Otsuka, H.; Stein, J. D.; Pacheco, A.; Peng, B.; Devarie-Baez, N. O.; Aguilar, H. C.; Lefer, D. J.; Xian, M., Controllable Hydrogen Sulfide Donors and Their Activity against Myocardial Ischemia-Reperfusion Injury. *ACS Chemical Biology* **2013,** *8* (6), 1283-1290.
25. Hirata, I.; Naito, Y.; Takagi, T.; Mizushima, K.; Suzuki, T.; Omatsu, T.; Handa, O.; Ichikawa, H.; Ueda, H.; Yoshikawa, T., Endogenous Hydrogen Sulfide Is an Anti-inflammatory Molecule in Dextran Sodium Sulfate-Induced Colitis in Mice. *Digestive Diseases and Sciences* **2011,** *56* (5), 1379-1386.
26. Yu, B. C.; Kang, T.; Xu, Y.; Liu, Y. Q.; Ma, Y. R.; Ke, B. W., Prodrugs of Persulfide and Sulfide: Is There a Pharmacological Difference between the Two in the Context of Rapid Exchanges among Various Sulfur Species In Vivo? *Angew. Chem. Int. Ed.* **2022**, 10.1002/anie.202201668.
27. Xu, S.; Wang, Y. Y.; Parent, Z.; Xian, M., Diacyl disulfides as the precursors for hydrogen persulfide ($H_2S_2$). *Bioorg. Med. Chem. Lett.* **2020,** *30* (4).
28. Sawa, T.; Takata, T.; Matsunaga, T.; Ihara, H.; Motohashi, H.; Akaike, T., Chemical Biology of Reactive Sulfur Species: Hydrolysis-Driven Equilibrium of Polysulfides as a Determinant of Physiological Functions. *Antioxid. Redox Signal.* **2022,** *36* (4-6), 327-336.
29. Levinn, C. M.; Cerda, M. M.; Pluth, M. D., Development and Application of Carbonyl Sulfide-Based Donors for $H_2S$ Delivery. *Acc. Chem. Res.* **2019,** *52* (9), 2723-2731.
30. Powell, C. R.; Dillon, K. M.; Wang, Y.; Carrazzone, R. J.; Matson, J. B., A Persulfide Donor Responsive to Reactive Oxygen Species: Insights into Reactivity and Therapeutic Potential. *Angew. Chem. Int. Ed.* **2018,** *57* (21), 6324-6328.
31. Marcolongo, J. P.; Venancio, M. F.; Rocha, W. R.; Doctorovich, F.; Olabe, J. A., NO/$H_2S$ "Crosstalk" Reactions. The Role of Thionitrites ($SNO^-$) and Perthionitrites ($SSNO^-$). *Inorg. Chem.* **2019,** *58* (22), 14981-14997.
32. Cortese-Krott, M. M.; Fernandez, B. O.; Kelm, M.; Butler, A. R.; Feelisch, M., On the chemical biology of the nitrite/sulfide interaction. *Nitric Oxide Biol. Chem* **2015,** *46*, 14-24.
33. Cortese-Krott, M. M.; Kuhnle, G. G. C.; Dyson, A.; Fernandez, B. O.; Grman, M.; DuMond, J. F.; Barrow, M. P.; McLeod, G.; Nakagawa, H.; Ondrias, K.; Nagy, P.; King, S. B.; Saavedra, J. E.; Keefer, L. K.; Singer, M.; Kelm, M.; Butler, A. R.; Feelisch, M., Key bioactive reaction products of the NO/$H_2S$ interaction are S/N-hybrid species, polysulfides, and nitroxyl. *Proc. Natl. Acad. Sci. USA* **2015,** *112* (34), E4651-E4660.

34. Wedmann, R.; Zahl, A.; Shubina, T. E.; Durr, M.; Heinemann, F. W.; Bugenhagen, B. E. C.; Burger, P.; Ivanovic-Burmazovic, I.; Filipovic, M. R., Does Perthionitrite ($SSNO^-$) Account for Sustained Bioactivity of NO? A (Bio)chemical Characterization. *Inorg. Chem.* **2015,** *54* (19), 9367-9380.

35. Filipovic, M. R.; Miljkovic, J. L.; Nauser, T.; Royzen, M.; Klos, K.; Shubina, T.; Koppenol, W. H.; Lippard, S. J.; Ivanovic-Burmazovic, I., Chemical Characterization of the Smallest S-Nitrosothiol, HSNO; Cellular Cross-talk of $H_2S$ and S-Nitrosothiols. *J. Am. Chem. Soc.* **2012,** *134* (29), 12016-12027.

36. Boulegue, J., Solubility of Elemental Sulfur in Water at 298 K. *Phosphorus and Sulfur and the Related Elements* **1978,** *5* (1), 127-128.

37. Ida, T.; Sawa, T.; Ihara, H.; Tsuchiya, Y.; Watanabe, Y.; Kumagai, Y.; Suematsu, M.; Motohashi, H.; Fujii, S.; Matsunaga, T.; Yamamoto, M.; Ono, K.; Devarie-Baez, N. O.; Xian, M.; Fukuto, J. M.; Akaike, T., Reactive cysteine persulfides and S-polythiolation regulate oxidative stress and redox signaling. *Proceedings of the National Academy of Sciences of the United States of America* **2014,** *111* (21), 7606-7611.

38. Fukuto, J. M.; Ignarro, L. J.; Nagy, P.; Wink, D. A.; Kevil, C. G.; Feelisch, M.; Cortese-Krott, M. M.; Bianco, C. L.; Kumagai, Y.; Hobbs, A. J.; Lin, J.; Ida, T.; Akaike, T., Biological hydropersulfides and related polysulfides - a new concept and perspective in redox biology. *Febs Lett.* **2018,** *592* (12), 2140-2152.

39. Duan, P. C.; Wang, Z. Y.; Chen, J. H.; Yang, G.; Raptis, R. G., Trigonal prismatic Cu(I) and Ag(I) pyrazolato nanocage hosts: encapsulation of $S_8$ and hydrocarbon guests. *Dalton Trans.* **2013,** *42* (42), 14951-14954.

40. Matsuno, S.; Yamashina, M.; Sei, Y.; Akita, M.; Kuzume, A.; Yamamoto, K.; Yoshizawa, M., Exact mass analysis of sulfur clusters upon encapsulation by a polyaromatic capsular matrix. *Nat. Commun.* **2017,** *8*, 749.

41. Bolton, S. G.; Pluth, M. D., Modified cyclodextrins solubilize elemental sulfur in water and enable biological sulfane sulfur delivery. *Chemical Science* **2020,** *11* (43), 11777-11784.

42. Bolton, S. G.; Pluth, M. D., Efficient inhibition of glyceraldehyde-3-phosphate dehydrogenase (GAPDH) by sulfuration with solubilized elemental sulfur. *Free Radical Biology and Medicine* **2022,** *185*, 46-51.

43. Brown, E. M.; Bowden, N. B., Stabilities of Three Key Biological Trisulfides with Implications for Their Roles in the Release of Hydrogen Sulfide and Bioaccumulation of Sulfane Sulfur. *ACS Omega* **2022,** *7* (13), 11440-11451.

44. Wheate, N. J.; Buck, D. P.; Day, A. I.; Collins, J. G., Cucurbit[n]uril binding of platinum anticancer complexes. *Dalton Trans.* **2006,** (3), 451-458.

45. Dong, N.; Xue, S.-F.; Zhu, Q.-J.; Tao, Z.; Zhao, Y.; Yang, L.-X., Cucurbit[n]urils (n=7, 8) binding of camptothecin and the effects on solubility and reactivity of the anticancer drug. *Supramolecular Chemistry* **2008,** *20* (7), 663-671.

46. Zhao, Y.; Buck, D. P.; Morris, D. L.; Pourgholami, M. H.; Day, A. I.; Collins, J. G., Solubilisation and cytotoxicity of albendazole encapsulated in cucurbit[n]uril. *Organic & Biomolecular Chemistry* **2008,** *6* (24), 4509-4515.

47. Deng, C.-L.; Murkli, S. L.; Isaacs, L. D., Supramolecular hosts as in vivo sequestration agents for pharmaceuticals and toxins. *Chem. Soc. Rev.* **2020,** *49* (21), 7516-7532.

48. Uzunova, V. D.; Cullinane, C.; Brix, K.; Nau, W. M.; Day, A. I., Toxicity of cucurbit[7]uril and cucurbit[8]uril: an exploratory in vitro and in vivo study. *Organic & Biomolecular Chemistry* **2010,** *8* (9), 2037-2042.

49. Thuéry, P., Lanthanide Complexes with Cucurbit[n]urils (n = 5, 6, 7) and Perrhenate Ligands: New Examples of Encapsulation of Perrhenate Anions. *Inorganic Chemistry* **2009,** *48* (10), 4497-4513.

50. Lin, R.-L.; Dong, Y.-P.; Tang, M.; Liu, Z.; Tao, Z.; Liu, J.-X., Selective Recovery and Detection of Gold with Cucurbit[n]urils (n = 5–7). *Inorganic Chemistry* **2020,** *59* (6), 3850-3855.

51. Mecozzi, S.; Rebek, J., Julius, The 55 % Solution: A Formula for Molecular Recognition in the Liquid State. *Chemistry – A European Journal* **1998,** *4* (6), 1016-1022.

52. Gomes, A. C.; Magalhães, C. I. R.; Oliveira, T. S. M.; Lopes, A. D.; Gonçalves, I. S.; Pillinger, M., Solid-state study of the structure and host–guest chemistry of cucurbituril-ferrocene inclusion complexes. *Dalton Transactions* **2016,** *45* (42), 17042-17052.

53. Steudel, R.; Jensen, D.; Göbel, P.; Hugo, P., Optical Absorption Spectra of the Homocyclic Sulfur Molecules Sn (n = 6, 7, 8, 9, 10, 12, 15, 20) in Solution [1]. *Berichte der Bunsengesellschaft für physikalische Chemie* **1988,** *92* (2), 118-122.

54. Connors, K. A., *Binding Constants: The Measurement of Molecular Complex Stability*. Wiley: 1987.

55. Miao, X. Q.; Li, Y.; Wyman, I.; Lee, S. M. Y.; Macartney, D. H.; Zheng, Y.; Wang, R. B., Enhanced in vitro and in vivo uptake of a hydrophobic model drug coumarin-6 in the presence of cucurbit 7 uril. *MedChemmComm* **2015,** *6* (7), 1370-1374.

56. Li, M.; Lee, A.; Kim, S.; Shrinidhi, A.; Park, K. M.; Kim, K., Cucurbit 7 uril-conjugated dyes as live cell imaging probes: investigation on their cellular uptake and excretion pathways. *Org. Biomol. Chem.* **2019,** *17* (25), 6215-6220.

57. Bockus, A. T.; Smith, L. C.; Grice, A. G.; Ali, O. A.; Young, C. C.; Mobley, W.; Leek, A.; Roberts, J. L.; Vinciguerra, B.; Isaacs, L.; Urbach, A. R., Cucurbit 7 uril-Tetramethylrhodamine Conjugate for Direct Sensing and Cellular Imaging. *J. Am. Chem. Soc.* **2016,** *138* (50), 16549-16552.

58. Montes-Navajas, P.; González-Béjar, M.; Scaiano, J. C.; García, H., Cucurbituril complexes cross the cell membrane. *Photochemical & Photobiological Sciences* **2009,** *8* (12), 1743-1747.

59. Chen, W.; Liu, C.; Peng, B.; Zhao, Y.; Pacheco, A.; Xian, M., New fluorescent probes for sulfane sulfurs and the application in bioimaging. *Chemical Science* **2013,** *4* (7), 2892-2896.

60. Moest, R. R., Hydrogen sulfide determination by the methylene blue method. *Anal. Chem.* **1975,** *47* (7), 1204-1205.

61. Kemp, S.; Wheate, N. J.; Stootman, F. H.; Aldrich-Wright, J. R., The Host-Guest Chemistry of Proflavine with Cucurbit[6,7,8]urils. *Supramolecular Chemistry* **2007,** *19* (7), 475-484.

62. Shen, X.; Kolluru, G. K.; Yuan, S.; Kevil, C. G., Chapter Two - Measurement of $H_2S$ In Vivo and In Vitro by the Monobromobimane Method. In *Methods in Enzymology*, Cadenas, E.; Packer, L., Eds. Academic Press: 2015; Vol. 554, pp 31-45.

63. Ditrói, T.; Nagy, A.; Martinelli, D.; Rosta, A.; Kožich, V.; Nagy, P., Comprehensive analysis of how experimental parameters affect H2S measurements by the monobromobimane method. *Free Radical Biology and Medicine* **2019,** *136*, 146-158.

64. Greiner, R.; Palinkas, Z.; Basell, K.; Becher, D.; Antelmann, H.; Nagy, P.; Dick, T. P., Polysulfides Link $H_2S$ to Protein Thiol Oxidation. *Antioxid. Redox Signal.* **2013,** *19* (15), 1749-U122.

65. Ono, K.; Akaike, T.; Sawa, T.; Kumagai, Y.; Wink, D. A.; Tantillo, D. J.; Hobbs, A. J.; Nagy, P.; Xian, M.; Lin, J.; Fukuto, J. M., Redox chemistry and chemical biology of $H_2S$, hydropersulfides, and derived species: Implications of their possible biological activity and utility. *Free Radic. Biol. Med.* **2014,** *77*, 82-94.

TOC Graphic:

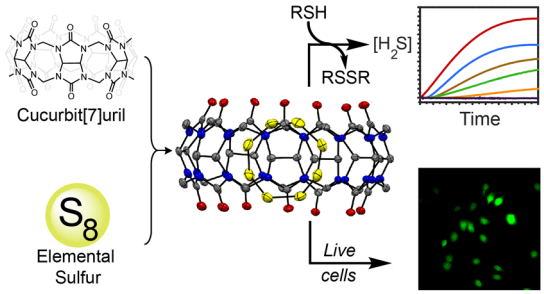


***Mechanism of $S_8$ reduction in CB[7] host-guest complexes***